Integration of second-life battery packs for self-consumption applications: analysis of a real experience

Adrian Soto[1], Alberto Berrueta[1], Pablo Zorrilla[1], Alvaro Iribarren[1], Diego H. Castillo[2], Wenceslao E. Rodríguez[2], Adolfo J. Rodríguez[2], David T. Vargas[2], Ignacio R. Matias[1], Pablo Sanchis[1], Alfredo Ursúa[1]

[1]*Department of Electrical, Electronic and Communication Engineering*

Institute of Smart Cities, Public University of Navarra

Pamplona, Spain

[2]*Master of Science and Computational Technologies, Academy of Computational Systems, Reynosa Rodhe Multidisciplinary Academic Unit-Autonomous University of Tamaulipas*

Reynosa, Mexico

Corresponding author: alfredo.ursua@unavarra.es

Abstract*—This contribution presents a methodology for the direct integration of Li-ion batteries discarded from electric vehicle into a collective self-consumption installation, showing the technical feasibility of such battery second use. In this regard, the state of charge (SOC) estimation is a relevant issue for the energy management of the second-life battery. Therefore, a *SOC* estimator is proposed in this contribution and tested in field. Moreover, the revealed costs analysis allows an economic comparison between the direct integration of a discarded battery pack in a second-life application or a remanufacture of these packs, thereby selecting the most suitable cells to build second-life batteries. This is a crucial issue for companies focused on the development of second-life batteries. The results obtained after testing the second-life battery system proposed in this contribution in a real installation make it possible to extol the benefits of including this type of batteries in a self-consumption system, reaching a self-consumption ratio of 69 % and reducing by 36 % the maximum power peak demanded from the grid.

Keywords*—battery, energy storage system, lithium-ion, second-life, SOC.

I. INTRODUCTION

Fighting against climate change has been considered as a primordial goal by United Nations (UN) [1]. To this end, the energy sector is expected to progressively change to cleaner production systems. Renewable energies, chiefly solar and wind generation, have been put forward as the best alternative to fossil fuels, reducing the amount of CO_2 particles emitted into the atmosphere. Green energies, in tandem with the decarbonization of the transport sector, make it possible to glimpse a future based on a sustainable development. Nevertheless, there exist some technical challenges that still need to be overcome.

On the one hand, the intermittence of the renewable sources can jeopardize the stability of the electricity grid [2]. Additionally, the power source is not available at our own whim. Therefore, renewable energies must be hybridized with energy storage systems. Lithium-ion batteries (LIBs) are commonly proposed as the best electrochemical storage system for stationary applications due to their high efficiency, fast dynamics and high cyclability [3].

On the other hand, the electrification of the transport sector brings a considerable hitch, the batteries used in the electric vehicles are replaced when the performance is depleted, mainly related with the capacity fade, generating an undesirable amount of waste. Furthermore, we cannot ignore the fact that the amount of minerals used for manufacturing batteries is limited and might be located in few areas.

Nonetheless, both concerns can be straddled to find a mutual solution. LIBs are discarded from the EVs when they do not comply with the exigent requirements of the automotive sector, typically when the state of health (SOH) reaches a threshold close to 70 %. However, they can be granted with a second-life for stationary applications [4], [5], encouraging the circular economy.

For that purpose, there exist three main solutions, the first of them relays on disassembling the battery packs and merging the cells with similar parameters such as capacity, internal resistance and self-discharge for reassembling them afterward. The main drawback of this method is the large amount of time invested in the characterization of all the cell/modules included in an EV battery pack [6]. Moreover, this method can be highly demanding of manual labor, driving up the expenses of the process.

The second method is based on developing an advanced battery management system (BMS). The modules extracted from the battery packs are batched independently of their *SOH*. The BMS is then the responsible for maximizing the charge delivered by the reassembled battery by bypassing the modules with lower performance. In such a way the capacity of the second-life battery can be enhanced up to a 30 % [7]. The main drawbacks of this method are that the energy density is reduced, and the high cost of the advanced BMS.

The third method, the one studied in this contribution, attempt to minimize the cost of second-life batteries by means of their direct integration, avoiding the disassembling process. As the BMSs of the EVs are not designed for working with PV inverters and for stationary applications, there are some challenges to surmount.

This work has been supported by the Spanish State Research Agency (AEI) under grants PID2019-111262RB-I00 /AEI/ 10.13039/501100011033 and DPI2016–80641-R, the European Union under the H2020 project STARDUST (774094), the Government of Navarra through research project 0011–1411–2018–000029 GERA and the Public University of Navarra under project ReBMS PJUPNA1904. Also noteworthy is the support received from the Mexican Program for Strengthening Educational Quality (PFCE) (2017-2021) for the Postgraduate Program Master of Science and Computational Technologies attached to the UAMRR-UAT.

XXX-X-XXXX-XXXX-X/XX/$XX.00 ©20XX IEEE

Firstly, the BMS integrated in the battery pack cannot communicate directly with the inverter; therefore, a liaison device must be included. Furthermore, this device must incorporate the start-up sequence, including the control of the precharge circuit. Secondly, given that the battery can be considered a black box, since the sensors and the balancing circuit cannot be modified or calibrated, a stochastic state of charge (SOC*)* estimator must be included in the liaison device, preventing the errors induced by the sensors. Those issues will be properly addressed in the upcoming sections.

This contribution develops a plug&play device and the required *SOC* estimation algorithm required for the direct connection of a battery pack discarded from an electric vehicle into a collective self-consumption system. Finally, experimental results measured from the operation of the second-life battery with the proposed liaison device in a collective self-consumption installation are presented, thereby validating the proposed device as well as the *SOC* estimation algorithm.

The contribution is organized as follows. Section II describes the developed liaison device. Section III presents the proposed *SOC* estimator. Section IV offers a description of the second-life battery pack and the scenario under study based on collective self-consumption of four homes. In Section V the main results are presented and discussed. Finally, in Section VI the main conclusions are summed up.

II. Development of the Liaison Device

As mentioned above, the BMS included in EV battery packs is merely designed for communicating with the electronic control unit (ECU) of the vehicle. Therefore, the first step in order to carry out the direct integration of second-life battery packs in micro grids or self-consumption applications is to develop a liaison device to establish the communication between the power inverter and the BMS. In the following lines, we describe the plug&play device for second-life batteries (PD4SB) developed in this contribution by means of standardized commercial solutions.

The first requirement of the PD4SB is to achieve a plug&play device, which means no configuration to be required when connecting it, as well as a minimum number of inputs and outputs. In the case of the PD4SB developed in this contribution, as it can be seen in Fig. 1, there is only a socket for the power supply, an RJ-45 connector for the communication with the inverter, an 8-pin connector for communicating with the BMS and a 24 V source for controlling a contactor. Moreover, it includes a start/stop button and 5 LEDs in order to indicate the state, which can be, normal operating (green), error (red), parameter out of limit (blue), warning (yellow) or starting protocol (yellow).

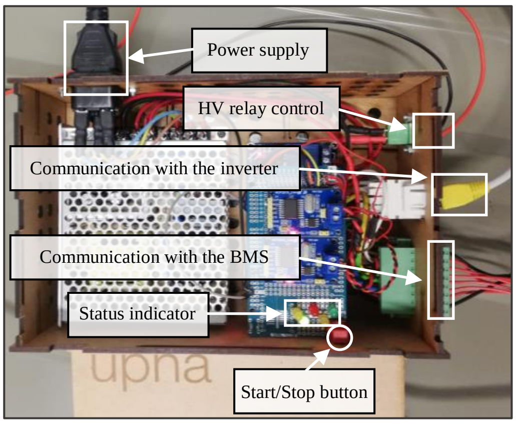

Fig. 1. Picture of the PD4SB liaison device.

For developing the PD4SB, an Arduino Mega 2560 microcontroller board has been used, the huge amount of information available, the user-friendly interface and the large number of compatible shields make it suitable for this application. The communication between the inverter and the BMS has been carried out by means of two CAN-BUS Shield v1.2. Firstly, the BMS send the information corresponding to the measurements of battery voltage, current and temperature to the Arduino, as well as the operating limits. Afterwards, the data are processed by the Arduino and sent to the inverter, following the CAN-BUS protocol defined by each manufacturer. It is worth noting that both, the BMS and the inverter have different baud rates, therefore Arduino needs to be a buffer.

For controlling the startup and shutting down sequences, an Arduino 4 Relay board in tandem with the PD4SL and the BMS has been used. Additionally, one of the relays is set to control an external high voltage and high current contractor, specifically an Omron G9EC-1 400 V 200 A DC Power Relay. The HV contactor is able to break the current flow if any error message is detected. Finally, an RT-65D AC-DC power source feeds the Arduino Mega and the relays.

It is worth noting that no additional sensor has been included. Thus, the *SOC* estimator has been developed to operate with the measurements of the BMS. The accuracy of those measurements is low (hundreds of mA, no more details about this inaccuracy can be provided due to confidentiality). Therefore, the *SOC* estimator needs to be robust against measurement inaccuracy.

III. *SOC* Estimator

There is a wide variety of *SOC* estimation algorithms, and the most suitable one depends on the application [8]. For instance, a typical battery designed for an automotive application does not operate continuously for more than 3 hours, and has long resting periods, when the electric vehicle is parked, thus, the cumulative error has not a crucial role and the *SOC* can be corrected when the car is parked or during the predefined and standardized charging process. However, a stationary battery may be cycled uninterruptedly for days, most likely, if it is designed for providing grid support services. Therefore, the *SOC* estimator designed for stationary applications should be robust in order to avoid the cumulative errors related with the measurement offsets. In addition, the computational requirements of the estimator need to be low enough to be implemented in a simple microprocessor. The most common *SOC* estimators are the Ampere-hour counting method and the electrical circuit model (ECM) estimator.

On the one hand, the Ampere-hour counting method is based on a current integration, as shown in (1).

$$SOC(\%) = SOC_{t0} - \int_{t_0}^{t} \frac{i_{bat}}{C} dt \cdot 100. \qquad (1)$$

This method is the simplest one but entails relevant inconveniences, as the entailed integral cumulative error. Furthermore, the capacity is considered as a constant value and it is not readjusted as the battery ages. Therefore, if the *SOC* is not periodically corrected large errors in the estimation can be reached, a deviation of a 10 % per day was observed when using this method in a stationary application [8].

On the other hand, the $V_{OC} – SOC$ relationship makes it possible to determine the *SOC* by measuring the open circuit voltage (V_{OC}). Nevertheless, the high current values reached in a stationary applications in tandem with the shifted internal resistance of second-life batteries reduce the accuracy of this method [8]. In the following lines, the estimator developed in this contribution is described.

The developed *SOC* estimator relays on a hybrid Ampere-hour counting method combined with an electrical circuit model (ECM) estimator. The main advantage of this estimator revolves around the low number of required inputs (only voltage and current), and the simplicity of the algorithm.

During the charging or discharging of the battery, the ampere-hour counting method is implemented. Afterwards, when a rest period is detected, the *SOC* is corrected by means of the $V_{OC} – SOC$ relationship. The rest of the battery is detected if the *SOC* variation is lower than 1 %/min and the battery current is lower than C/15. After 10 minutes of rest, the *SOC* is obtained by means of both, the Ampere-hour counting method and by the electrical model based on the relation between V_{OC} and *SOC*. In order to avoid sharp variations in the estimation, it is progressively corrected during the next 5 minutes, as expressed in (2).

$$SOC(\%) = SOC_{V_{oc}} \cdot \frac{k}{300} + SOC_{Ah} \cdot \frac{300-k}{300} \quad (2)$$

where $SOC_{V_{OC}}$ is the estimation of the electrical model, SOC_{Ah} is the estimation of the amper counting method and k is the time since the correction started. For resting periods longer than 15 minutes, the *SOC* is estimated by the electrical model, as shown in Fig. 2.

IV. Battery Characterization and Description of the System

In order to test the feasibility of second-life batteries as energy storage systems in a collective self-consumption scenario, a real second-life battery pack coming from a Nissan Leaf has been directly integrated into an experimental self-consumption system located at the Energy Storage and Microgrids Laboratory of the Public University of Navarra (UPNA), Spain, by means of the PD4SB described above.

A. Second-life battery characterization

An overall electrical model of the battery is required for the development of a *SOC* estimator, and the state of health of the battery needs to be assessed. The main electrical parameters of second-life LIB are presented in this subsection.

The testing methodology carried out for the measurement of electrical parameters is based on three consecutive charge – discharge cycles followed by a galvanostatic intermittent titration test (GITT). The three cycles pinpoint the current capacity, *SOH*, coulombic efficiency (η_C) and energy efficiency (η_E). The cycles were carried out at a C/3 constant current C-rate. Currents lower than C/3 avoid the self-heating of LIBs, ensuring the proper measurement of capacity [9]. C-rate is defined as the battery current over its rated capacity, as defined in (3). Coulombic efficiency is defined as (4) while energy efficiency is obtained means of (5). *SOH* is the main indicator of the aging of a LIB, and depicts the capacity loss, as calculated in (6)

$$C\text{-}rate = \frac{i_{bat}}{C_N} \quad (3)$$

$$\eta_C = \frac{C_{dishcarge}}{C_{charge}} \quad (4)$$

$$\eta_E = \frac{E_{discharge}}{E_{charge}} \quad (5)$$

$$SOH = \frac{C}{C_N} \quad (6)$$

where i_{bat} is the charge/discharge current, C_N is the rated capacity of the battery and C is the current capacity.

Capacity and energy obtained during the discharging process, as well as efficiency values are presented in Table I. It can be observed that the capacity rises during the first cycles. This phenomenon has been reported to appear in new batteries, and can be related to a resistance reduction [10]. However, to the best of our knowledge, the electrochemical mechanisms related to this phenomenon in second-life batteries has not been properly addressed.

The relationship between *SOC* and V_{OC} can be set based on the GITT. The relationship is obtained by measuring the voltage at different *SOC* levels. For the assurance of thermodynamic stabilization of the battery a 1 h rest period is set. V_{OC} is measured every ΔSOC of 10%, during both battery

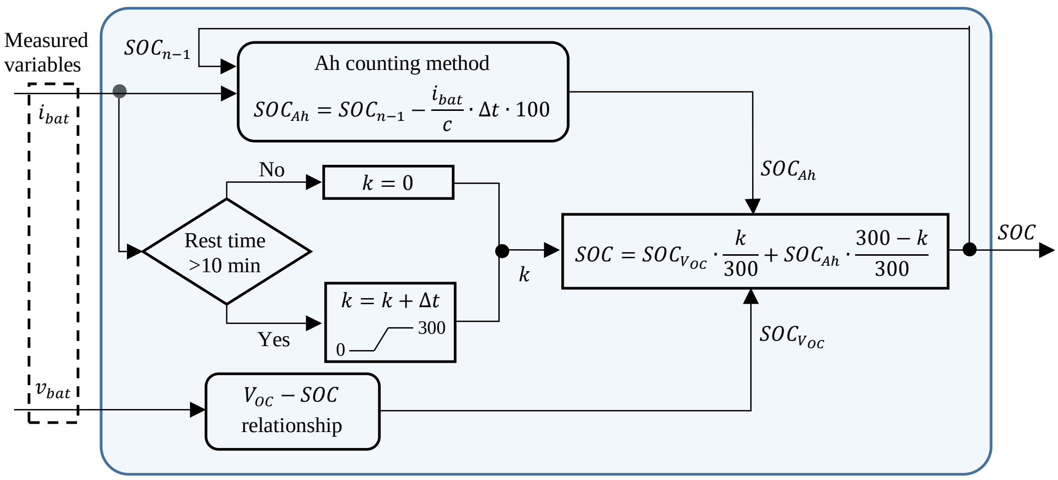

Fig. 2. Flowchart of the proposed *SOC* estimator.

charge and discharge. Not only does the GITT establish the *Voc– SOC* relationship, but also allows obtaining the inner resistance (R_{DC}) at different *SOC* levels. The proper quantification of the internal resistance is primordial in order to develop battery thermal models, since it allows to quantify the heating induced in the LIBs as function of the battery current, as the temperature is a crucial feature concerning the performance of LIBs [11]. The common form of obtaining R_{DC} is based on introducing a current step (ΔI) of 10 s, which leads to a voltage drop (ΔV). According to Ohm's law R_{DC} can be measured by means of (7)

$$R_{DC} = \frac{\Delta V}{\Delta I}. \quad (7)$$

The $V_{OC} – SOC$ relationship is presented in Fig. 3. A minimal hysteresis among the discharging points (left-pointing triangles) and the charging ones (right-pointing triangles) is measured. Hence, this relationship can be fitted by means of a 6th order polynomial, with no difference between charge and discharge. According to the goodness of fit, the results show an R^2 of 0.995 and a RMSE of 0.6 %.

TABLE I. CAPACITY AND EFFICIENCY RESULTS

	Cycle 1	Cycle 2	Cycle 3	Unit
Capacity	38.6	38.8	39	Ah
Energy	14.1	14.2	14.3	kWh
η_C	100	99.5	99.6	%
η_E	96.1	95.9	96.1	%
SOH	58.3	58.6	58.9	%

The measured R_{DC} values are constant for a *SOC* range of 20 – 90 %, and the difference between charging and discharging measurements is negligible. Nevertheless, a substantial growth is noticed at low *SOC*, lower than 20 %, where R_{DC} is increased by 63 %, as it can be observed in Fig. 4.

The characterization tests have been conducted in a controlled ambient of 23±3 °C. All the charge and discharge processes were conducted via a GEEL+30+HV manufactured by CINERGIA, in which the datalogger is included, the sampling frequency was set to 1 Hz.

B. Collective self-consumption system

The self-consumption system is being continuously monitored and managed by the power management system

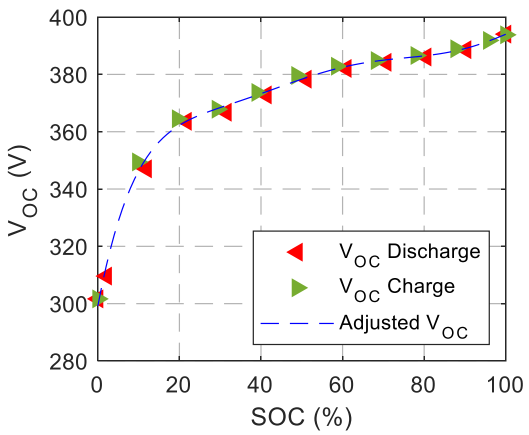

Fig. 3. $V_{OC} – SOC$ relationship.

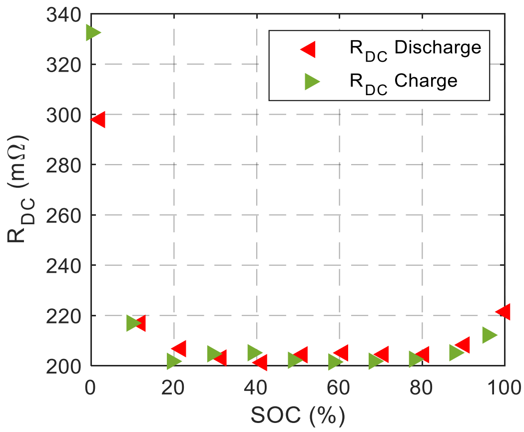

Fig. 4. R_{DC} measurements for different *SOC* values.

(PMS), in which the desired energy management strategy for the ESS can be set. In the case of this contribution, the strategy aims at a maximum self-consumption. The system includes an INGECON Sun Storage 6TL manufactured by INGETEAM, connected to an 11.5 kWp PV array. Given that the system is located at the Public University of Navarra, the power consumption is based on data measured in four homes located in the vicinity of the UPNA, as represented in Fig. 5. The equations that govern the operation of the self-consumption system are:

$$(P_{bat} + P_{PV}) \cdot \eta_{inv} = P_{inv} \quad (8)$$

$$P_{inv} + P_{grid} = P_{load} \quad (9)$$

where $\eta_{inv}$is the efficiency of the inverter. P_{load} is the total power demanded by the 4 homes, P_{inv} the power injected by the inverter and P_{grid} the power consumption from the electricity grid. According to the sign convention, P_{bat} and i_{bat} are positive when the battery is being discharged, as illustrated in Fig. 5.

The boundary conditions of the battery are summarized in Table II and the constraints of the battery and the system limitations are given by:

$$v_{bat,min} \leq v_{bat} \leq v_{bat,max} \quad (10)$$

$$SOC_{min} \leq SOC \leq SOC_{max} \quad (11)$$

$$abs(i_{bat}) \leq i_{bat,max} \quad (12)$$

$$P_{inv} > 0 \quad (13)$$

$$P_{grid} > 0 \quad (14)$$

TABLE II. BOUNDARY CONDITIONS

Parameter	Value	Unit
$v_{bat,min}$	302	V
$v_{bat,max}$	393	V
SOC_{min}	0	%
SOC_{max}	98	%
$i_{bat,max}$	20	A

As defined by the maximum self-consumption strategy the power inverter cannot charge the battery from the electrical

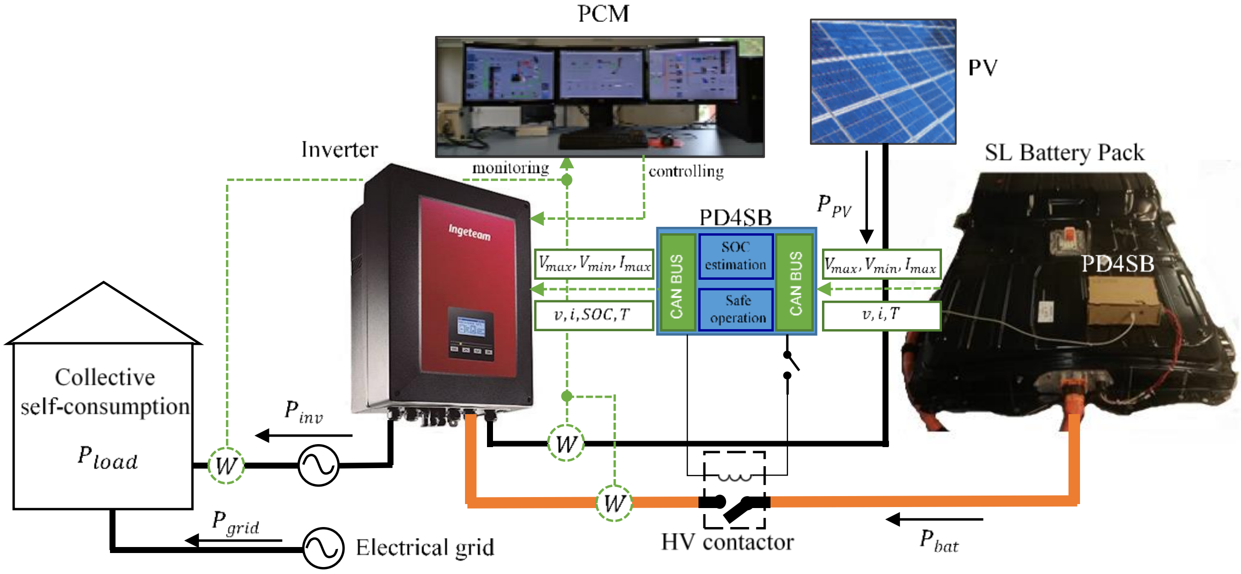

Fig. 5. Schematic representation of the integration of a second-life battery pack in the self-consumption system located at the Energy Storage and Microgrids Laboratory of the Public University of Navarra.

grid except when an emergency charge is required in order to prevent the irreparable damage of the battery, when the *SOC* is equal to zero the battery is charged up to a 2 % *SOC* at 500 W. Furthermore, we have considered that the energy surplus coming from the PV array cannot be injected into the grid, this issue can vary considering the legislative context of the country under studio.

V. On Field Validation and Discussion

The measurements corresponding to the operation of the collective self-consumption system for one week are presented in Fig. 6, more precisely the data were acquired from 16th to 23rd of February 2021. In the first graph the power balance is shown, the black line is the electricity consumption of four homes, which is supplied by the electrical grid (grey area), solar energy (orange area) or the second-life battery (green area), for the shake of clarity the battery charge is represented in yellow. The second graph shows the battery power and the third one corresponds to the *SOC* estimation. A detailed functioning of a single day, corresponding to February 18th can be seen in Fig. 7.

After one week of testing, the system operated as expected, proving the proper performance of a full battery pack coming from an EV as energy storage system in self-consumption applications. More precisely, the results show that the self-consumption ratio raised from 37 % to 69 % when it is compared to the same installation relaying only on PV generation without energy storage.

Moreover, the power peak provided by the electricity grid is reduced from 10.8 kW without self-consumption to 9.8 kW when it is based merely on PV generation and to 6.9 kW when the energy storage is included. The maximum peak of consumption corresponds to the evening period, with just PV generation, therefore, no substantial reduction of P_{grid} is observed. Depending on the electricity fee of the case study, the reduction in the maximum power coming from the grid could correspond to a considerable saving in the electricity bill. It is out of the scope of this contribution to quantify the profitability of including a second-life battery, since it

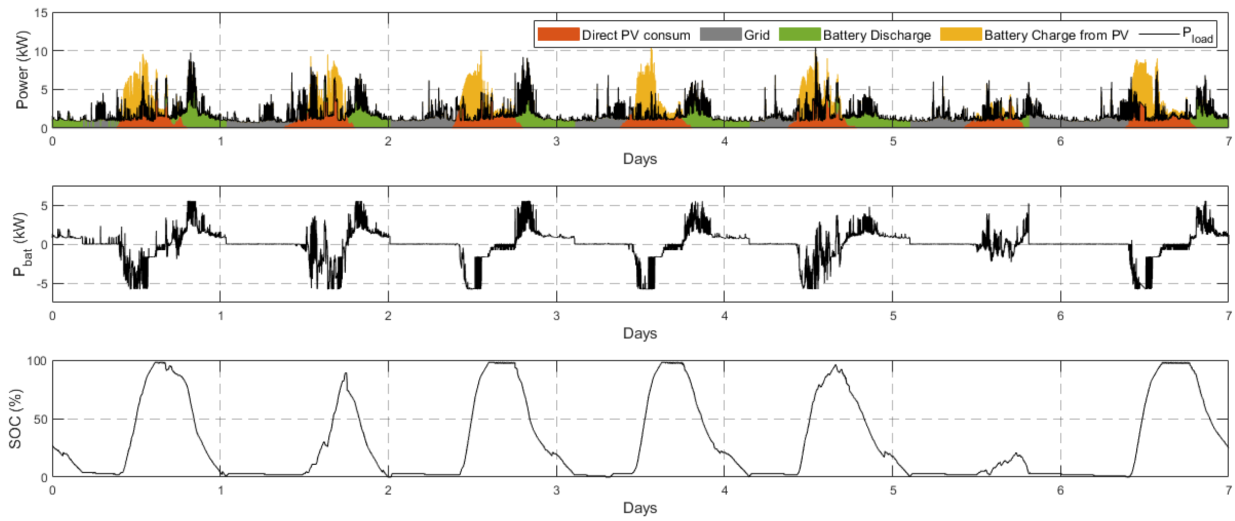

Fig. 6. Power balance of the self-consumption installation corresponding to February 16th to 23rd. Power balance of the second-life battery. Proposed *SOC* estimator results during a week of on field operation.

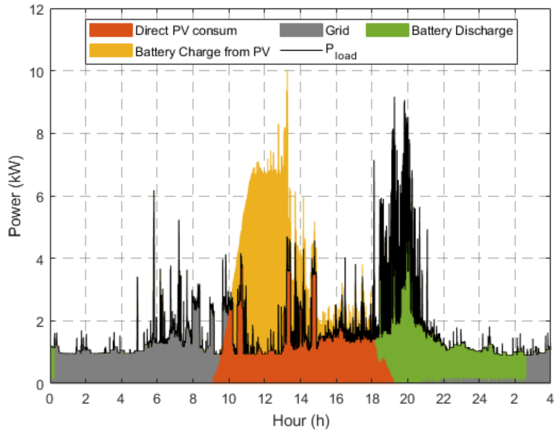

Fig. 7. Power balance corresponding to February 18th.

depends on the consumption profile, legislation and the economical context of the location.

The developed *SOC* estimator has been shown to avoid the cumulative error induced by current measurement offsets or inaccuracies. The deviations were corrected during night periods and when the battery was fully charged. Nevertheless, further research is needed in order to develop more accurate *SOC* estimators for second-life batteries that could enhance the performance of the battery, including dependency with the temperature and the ability to update the capacity value as the battery ages.

VI. Conclusions

This contribution shows the procedure and the technical feasibility of a direct integration of a battery pack discarded from an electric vehicle into a collective self-consumption installation. Furthermore, a *SOC* estimator has been developed and tested in field. Finally, the results obtained after a week of testing show the benefits of including a second-life battery in a self-consumption installation.

The developed liaison device, which allows the communication between the power inverter and the BMS, embedded in the battery pack has a total cost of € 335, a breakdown of the expenses is presented in Fig. 8. This device has been erected using standard commercial solution, as an Arduino Mega with several shields and a commercial AC – DC converter, therefore, it can be easily replicated. However, a company focused on second-life batteries can substantially reduce the cost of the device, particularly if the Arduino and the AC – DC converter are replaced by an ad-hoc solution, see that those devices involve a 25 % of the total cost. Furthermore, the component with a higher value is the HV contactor, which represents a 65 % of the total cost, depending on the system, this breaker is included in the inverter and it would not be necessary to include it in the liaison device. Hence, sharp improvements can be reached concerning the cost reduction of the liaison device, reducing the final price up to a 75 %. This fact shows up the direct integration of second-life batteries as a promising solution for on the one hand reducing the waste arisen by the electric vehicles and on the other hand as an affordable and eco-friendly energy storage system for enhancing the self-consumption.

Additionally, notwithstanding the advanced *SOH* of the battery, nearly a 60 %, the battery has shown a sterling efficiency, being η_C almost unitary and an energy efficiency higher than 95 %. Even being a second-life battery, its

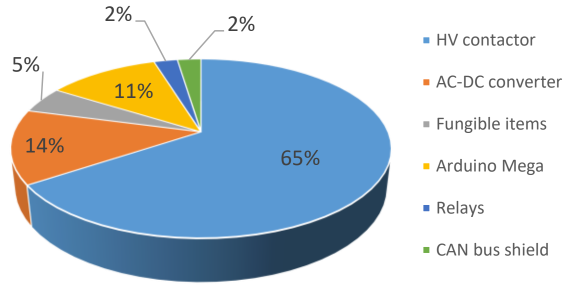

Fig. 8. Breakdown of the expenses of the liaison PD4SB.

efficiency is higher than other conventional energy storage systems such as lead-acid batteries or the ones based on hydrogen.

Secondly, the proposed *SOC* estimator has shown to avoid the cumulative error and to be able to prevent the possible errors induced by the uncertainty of the internal sensors included in the battery pack.

Finally, in this particular case, during a week of testing at the self-consumption system, the integration of a second-life battery has made it possible to reach a self-consumption ratio of 69 % and to reduce the maximum power peak from 10.8 to 6.9 kW in a four-homes collective self-consumption system.

References

[1] United Nations, “SUSTAINABLE DEVELOPMENT GOALS.” .

[2] I. de la Parra, J. Marcos, M. García, and L. Marroyo, “Dealing with the implementation of ramp-rate control strategies - Challenges and solutions to enable PV plants with energy storage systems to operate correctly,” *Solar Energy*, vol. 169, no. April, pp. 242–248, 2018.

[3] A. Berrueta, A. Soto, J. Marcos, I. De La Parra, P. Sanchis, and A. Ursua, “Identification of Critical Parameters for the Design of Energy Management Algorithms for Li-Ion Batteries Operating in PV Power Plants,” *IEEE Transactions on Industry Applications*, vol. 56, no. 5, pp. 4670–4678, 2020.

[4] E. Martinez-Laserna *et al.*, “Technical Viability of Battery Second Life: A Study from the Ageing Perspective,” *IEEE Transactions on Industry Applications*, vol. 54, no. 3, pp. 2703–2713, 2018.

[5] C. White, B. Thompson, and L. G. Swan, “Comparative performance study of electric vehicle batteries repurposed for electricity grid energy arbitrage,” *Applied Energy*, vol. 288, no. February, p. 116637, 2021.

[6] E. Braco, I. San Martín, A. Berrueta, P. Sanchis, and A. Ursúa, “Experimental assessment of cycling ageing of lithium-ion second-life batteries from electric vehicles,” *Journal of Energy Storage*, vol. 32, no. May, p. 101695, 2020.

[7] A. Berrueta, I. S. Martin, J. Pascual, P. Sanchis, and A. Ursua, “On the requirements of the power converter for second-life lithium-ion batteries,” *2019 21st European Conference on Power Electronics and Applications, EPE 2019 ECCE Europe*, pp. 1–8, 2019.

[8] A. Berrueta, I. San Martín, P. Sanchis, and A. Ursúa, “Comparison of State-of-Charge estimation methods for stationary Lithium-ion batteries,” *IECON Proceedings (Industrial Electronics Conference)*, pp. 2010–2015, 2016.

[9] A. Soto, A. Berrueta, P. Sanchis, and A. Ursua, “Analysis of the main battery characterization techniques and experimental comparison of commercial 18650 Li-ion cells,” *Proceedings - 2019 IEEE International Conference on Environment and Electrical Engineering and 2019 IEEE Industrial and Commercial Power Systems Europe, EEEIC/I and CPS Europe 2019*, pp. 1–6, 2019.

[10] M. Ecker, P. Shafiei Sabet, and D. U. Sauer, “Influence of operational condition on lithium plating for commercial lithium-ion batteries – Electrochemical experiments and post-mortem-analysis,” *Applied Energy*, vol. 206, no. August, pp. 934–946, Nov. 2017.

[11] J. Jaguemont, A. Nikolian, N. Omar, S. Goutam, J. Van Mierlo, and P. Van Den Bossche, “Development of a Two-Dimensional-Thermal Model of Three Battery Chemistries,” *IEEE Transactions on Energy Conversion*, vol. 32, no. 4, pp. 1447–1455, 2017.